J Biomol NMR (2014) 59:31–41
DOI 10.1007/s10858-014-9821-7

ARTICLE

Long-lived spin state of a tripeptide in stretched hydrogel

Kaz Nagashima · D. Krishna Rao · Guilhem Pagès · S. Sendhil Velan · Philip W. Kuchel

Received: 19 December 2013 / Accepted: 24 February 2014 / Published online: 14 March 2014

Abstract The longitudinal (T_1), transverse (T_2), and singlet state (T_s) relaxation times of the geminal backbone protons (CH_2) of L-Leu-Gly-Gly were studied by NMR spectroscopy at 9.4 T in a bovine hide gelatin gel composed in D_2O at 25 °C. Gelatin granules were dissolved in a hot solution of the tripeptide and then the solution was allowed to gel inside a flexible silicone tubing. With increases in gelatin content, the T_2 and T_s of the CH_2 protons correspondingly decreased ($T_s/T_2 \sim$ constant), while the change in T_1 was relatively small. The largest observed T_s/T_1 value was 3.3 at 46 % w/v gelatin that was the lowest gelatin content examined. Stretching the tubing, and hence the gel, brought about anisotropic alignment of the constituents resulting in residual quadrupolar splitting of the resonance from D_2O in ^2H NMR spectra, and residual dipolar splitting of the CH_2 resonance in ^1H NMR spectra. WALTZ-16 decoupling during the relaxation intervals extended the singlet state relaxation time, but the efficacy diminished as the gels were stretched. Theoretically predicted T_1, T_2, and T_s values, assuming intramolecular dipolar coupling as the only source of relaxation, were within the same order of magnitude as the experimentally observed values. Overall we showed that it is possible to observe a long-lived spin state in an anisotropic medium when T_2 is shorter than T_1 in the presence of non-zero residual dipolar couplings.

Keywords Singlet · Long-lived spin state · Relaxation · Aligned media · Stretchable gel

K. Nagashima (✉) · D. K. Rao · G. Pagès · S. S. Velan
Singapore Bioimaging Consortium, A*STAR, 11 Bioplis Way, Singapore 138667, Singapore
e-mail: kaznaga@sbic.a-star.edu.sg

P. W. Kuchel
School of Molecular Bioscience, University of Sydney, Sydney, NSW 2006, Australia

Introduction

Singlet spin states in the context of NMR, viz., a virtually nonmagnetic eigenstate formed by a pair of coupled spin-1/2 nuclei, were already known in the early 1970s (Hoffman et al. 1971). This somewhat long-forgotten spin state had not been explored further until 2004 when Carravetta et al. (2004) reported a relaxation time that was longer than the corresponding longitudinal relaxation time, T_1. The limit of quantum coherences, which was once believed to be no more than T_1, can be overcome by cancellation of intramolecular dipolar interactions, by forcing two coupled nuclear magnetic vectors to orient in opposite directions, and yet to precess at the same angular frequency to cancel the vector sum of the two magnetic moments (Levitt 2012). Such, so-called, long-lived spin states are now at the forefront of NMR research, with the expectation of yielding novel magnetic resonance imaging (MRI) contrast (Warren 2011; DeVience et al. 2013) and preserving hyperpolarized magnetization (Vasos et al. 2009; Tayler et al. 2012; Franzoni et al. 2012; Feng et al. 2012; Chen et al. 2013; Pileio et al. 2013).

The quintessence of the somewhat enigmatic quantum state is understood as follows. In the singlet–triplet basis, the wave functions for a coupled two-spin system ($|\alpha\alpha\rangle$, $|\alpha\beta\rangle$, $|\beta\alpha\rangle$ *and* $|\beta\beta\rangle$) can be rearranged to give

$$\psi^{ST} = \begin{bmatrix} |\alpha\alpha\rangle \\ (|\alpha\beta\rangle + |\beta\alpha\rangle)/\sqrt{2} \\ (|\alpha\beta\rangle - |\beta\alpha\rangle)/\sqrt{2} \\ |\beta\beta\rangle \end{bmatrix} = \begin{bmatrix} |T_{+1}\rangle \\ |T_0\rangle \\ |S_0\rangle \\ |T_{-1}\rangle \end{bmatrix} \quad (1)$$

where the $|T_M\rangle$ represents triplet states, $|S_0\rangle$ a singlet state, and their subscripts the sum of the spin quantum numbers ($M = \Sigma m_I$ in which $m_I = +1/2$ for α and $-1/2$ for β).

The Schrödinger equation for a coupled two-spin system can therefore be written as follows (Levitt 2011 pp 357–361):

$$H^{\mathrm{ST}}\Psi^{\mathrm{ST}} = \frac{1}{2}\begin{bmatrix} \omega_1+\omega_2+\pi J+d & 0 & 0 & 0 \\ 0 & \pi J-2d & \omega_1-\omega_2 & 0 \\ 0 & \omega_1-\omega_2 & -3\pi J & 0 \\ 0 & 0 & 0 & -(\omega_1+\omega_2)+\pi J+d \end{bmatrix}\begin{bmatrix} |T_{+1}\rangle \\ |T_0\rangle \\ |S_0\rangle \\ |T_{-1}\rangle \end{bmatrix} \quad (2)$$

where ω_1 and ω_2 are the Lamor frequencies of Spin 1 and Spin 2, and J and d are the scalar and dipolar coupling constants, respectively. If the two spins are forced to precess at the same frequency, $\omega_1 = \omega_2$, the Hamiltonian matrix for the coupled two spins becomes diagonal and the four spin states are quantized independently of each other. Another important point here is that the eigenvalue of the singlet state, viz.,

$$H^{\mathrm{ST}}|S_0\rangle = \left(-\frac{3\pi J}{2}\right)|S_0\rangle\,, \quad (3)$$

does not contain a d term in it, which means the cancellation of the intramolecular dipolar interaction. In other words, because of the antisymmetry of the singlet states with respect to spin exchange, intramolecular dipole–dipole relaxation becomes inoperative on the singlet state. This results in enhancement of the lifetime of the state beyond T_1, which was once believed to constitute the unchangeable time limit on 'spin memory'.

Hydrogels have been used for resolving overlapping resonances by use of dipolar splittings in liquid-state NMR spectroscopy (Bax 2003). Currently, such gel NMR experiments can be done with available commercial glass tubes and plastic kits specially designed for gel-NMR (New Era Enterprises 2012–2013). Furthermore, mechanical extension of hydrogels supported in silicone tubing has been applied in NMR studies (Kuchel et al. 2006) in order to control anisotropy parameters, such as residual dipolar coupling (Kummerlöwe et al. 2008; Kummerlöwe and Luy 2009), quadrupolar coupling (Naumann et al. 2007) and chemical shift anisotropy (Hallwass et al. 2011). By stretching or compressing a gel in a polymer tubing, molecular alignment of guest molecules takes place along the axial and radial directions, respectively. The extent of the dipolar interaction between two nuclear spins is determined by

$$d = -\frac{\mu_0}{4\pi}\frac{\gamma^2\hbar}{r^3}\frac{\langle 3\cos^2\theta_{\mathrm{DP}}-1\rangle}{2} = b\,\frac{\langle 3\cos^2\theta_{\mathrm{DP}}-1\rangle}{2} \quad (4)$$

where μ_0 is the permeability of a vacuum, γ the magnetogyric ratio of the two nuclei, r the distance between them, $\hbar$ (= $h/2\pi$) the reduced Planck's constant, b the dipolar coupling constant, and θ_{DP} the angle between the internuclear vector and the static magnetic field, $\mathbf{B}_0$. The angled brackets denote the average over all orientations of the internuclear vector. From Eqs. (3) and (4), ignoring all relaxation mechanisms other than that due to intramolecular dipolar interactions, it is expected that singlet-state relaxation will not be affected by a change in the value of d that can be brought about by stretching the gel. Thus, it is of interest if singlet states can be observed in an aligned medium in which residual dipolar interactions are manually adjustable. Also, a stretched gel is a model of fibrous tissues so these samples can be useful for developing approaches for exploiting singlet states in vivo.

A limited number of NMR/MRI studies have envisaged the use of singlet states for in vivo applications (Ghosh et al. 2011; Laustsen et al. 2012; Pileio et al. 2013; Zhang et al. 2013). Evaluation of the feasibility of using singlet states to probe metabolic responses in cells and tissues was a major aim of the present study (and in line with the thrust of our Institute). We chose L-Leu-Gly-Gly as a guest species in stretchable gels because similar di- and tri-peptides have been shown to form singlet-states in aqueous solution (Tayler and Levitt 2011a, b). It was dissolved in a hot gelatinous fluid and the solution was allowed to gel in a flexible silicone tubing at room temperature. The stretchable tubing was inserted into a bottomless 5-mm o.d. NMR tube and lowered into a standard high resolution NMR probehead. The relaxation of a pair of geminal ^{1}H nuclei of the tripeptide was studied in the aligned medium systematically at various gelatin concentrations and extents of stretching. To our knowledge this is the first report of eliciting a nuclear magnetic singlet state in the presence of a non-zero residual dipolar coupling, in a very viscous medium.

Materials and methods

L-Leu-Gly-Gly (0.1 g; L-leucylglycylglycine Sigma-Aldrich) was first dissolved in D_2O (1.2 g; Cambridge Isotopes). A specified amount (0.50–0.65 g) of bovine hide gelatin powder (Gelita, Brisbane, QLD, Australia, Lot # 80 32 256) was weighed and added to the solution. The mixture was heated to 75 °C using a thermostated hotplate and thoroughly vortex-mixed to homogenize the viscous gel matrix. The particular tripeptide was found to be stable in the hot gelatin solutions. The solution was frozen in liquid nitrogen, vacuum-pumped, and redissolved at 75 °C. The same freeze–pump–thaw cycle was repeated three times to eliminate dissolved oxygen. The solution was reheated to 75 °C to liquefy, and was then drawn into the silicone tubing (Dow Corning SILASTIC® lab tubing; Cat # 508-009; 1.98 mm i.d., 3.18 mm o.d.) using a disposable plastic syringe, and allowed to gel at room temperature. The open ends of the silicone tubing were capped with plastic plugs to retain the water contents. The round-bottom part of a 5-mm thick-walled glass NMR tube (Wilmad, Buena, NJ, USA, 524 pp or Norell, Landisville, NJ, USA, S-5-500) was cut off after scoring with a sharp steel file. The gel tubing was fixed in the bottomless NMR tube with a plastic plug at its lower end (Kuchel et al. 2006). The stretched length of the gel was adjusted with a plastic thumb-screw resting on the top of the glass sample tube.

A Bruker Avance III 400 MHz NMR spectrometer was used with the sample temperature set to 25.0 °C, in an indirect-detection liquid NMR probe, inside a 54-mm standard-bore Bruker 9.4 T magnet. The ^{1}H 90° pulse duration was calibrated to be 9.3 μs, at a transmitter power of 10 W. The spectrometer frequency was locked on the ^{2}H resonance in D_2O during all measurements by readjusting the frequency and sweep settings after each gel-stretching step. The transmitter offset frequency was also readjusted to the center of the proton resonance of interest (vide infra) after each stretching. A series of experiments [one dimensional (1D), T_1, T_s, T_2, and diffusion] were run consecutively with a relaxation delay of 10 s, which assured 10 × T_1 times had elapsed before each subsequent transient. For acquiring 1D spectra, a single 90° pulse was used; and for T_1 measurements a conventional inversion recovery pulse sequence was used. For T_s measurements, the M2S-S2M sequence (Pileio et al. 2010; Feng et al. 2012) was used with an echo interval $\tau = 15$–5 ms, from zero to maximum gel extension, with fixed loop counts of $n_1 = 3$, for which the best interval value was calibrated in trial experiments. These experimentally determined parameters corresponded well to theoretical prediction given by $\tau = (\pi/2)/\sqrt{(2\pi J - d)^2 + (2\pi \Delta\nu)^2}$ and $n_1 = (\pi/2)/\tan^{-1}(2\pi\Delta\nu/(2\pi J - d))$ (Torres et al. 2012). The first 90° pulse (and receiver phase as a result) of the sequence was inverted in each transient in order to cancel out relaxed magnetization. The efficiency of conversion from the original magnetization ($I_x + S_x$) to the singlet state depends on the chemical shift difference ($\Delta\nu$) and the couplings ($d/2\pi$, J). In our particular case, ignoring relaxation, when $d = 0$, density matrix calculations (Pileio et al., 2010) predict its 90.8 % conversion to $ZQ_x = (1/2)\ (|T_0\rangle\langle T_0| - |S_0\rangle\langle S_0|)$ during the M2S step. For T_2 measurements, since spectral modulation due to the total coupling ($T = J + d$) interfered with accurate estimation of the relaxation time constant, a CPMG pulse sequence with a 'magic-echo' for J-suppression (Aguilar et al. 2012) was used, incrementing the even-numbered loop counts at a constant pulse interval of 2.5 ms. For diffusion measurements a bipolar stimulated echo pulse sequence (Wu et al. 1995; Pelta et al. 1998) was used with a diffusion time $\Delta = 0.5$ s and rectangular gradient pulse duration of $\delta/2 = 1.5$ ms. In all of the above NMR experiments, eight transients were accumulated per spectrum. The samples were studied in sequence from original unstretched length to maximum length, in order to mitigate influences from possible hysteresis in extension and shrinkage processes. Also, the stretched-gel samples were run soon after extension in the NMR laboratory, ignoring possible slow equilibration due to thixotropy. The ^{2}H NMR spectra of D_2O in the gel were observed through the lock channel of the NMR probehead at 2.5 W radiofrequency (RF) power and 100 μs duration pulse by reconfiguring the wiring to a broadband preamplifier and receiver after the lock had been turned off.

Results

Figure 1 shows a ^{1}H NMR spectrum from a hydrogel of 46 % w/v gelatin with incrementing the extension factor. In the present work, the extension factor (f_E) is defined as

$$f_E \equiv \frac{1}{1 - \frac{\Delta L_R}{L_{tube}}}, \tag{5}$$

where ΔL_R is the extra length of gel-filled tubing measured above the bottomless NMR tube (L_{tube}) with no tension. In this study $\Delta L_R = 0$–77 mm (variable), $L_{tube} = 134$ mm (constant), and $f_E \geq 1$. All of the spectra were internally referenced to HDO at 4.70 ppm. Each geminal proton pair in the two Gly residues ("a" and "b" protons) showed the characteristic 'tilted-roof' line shape typical of an AB coupled spin system (Reich 2013). The two geminal protons are nearly magnetically equivalent but have slightly different chemical shifts (Taylor and Levitt 2011a, b) probably due to constraints in the backbone crank motion (Tonan and Ikawa 2003; Barfield et al. 1976). The central

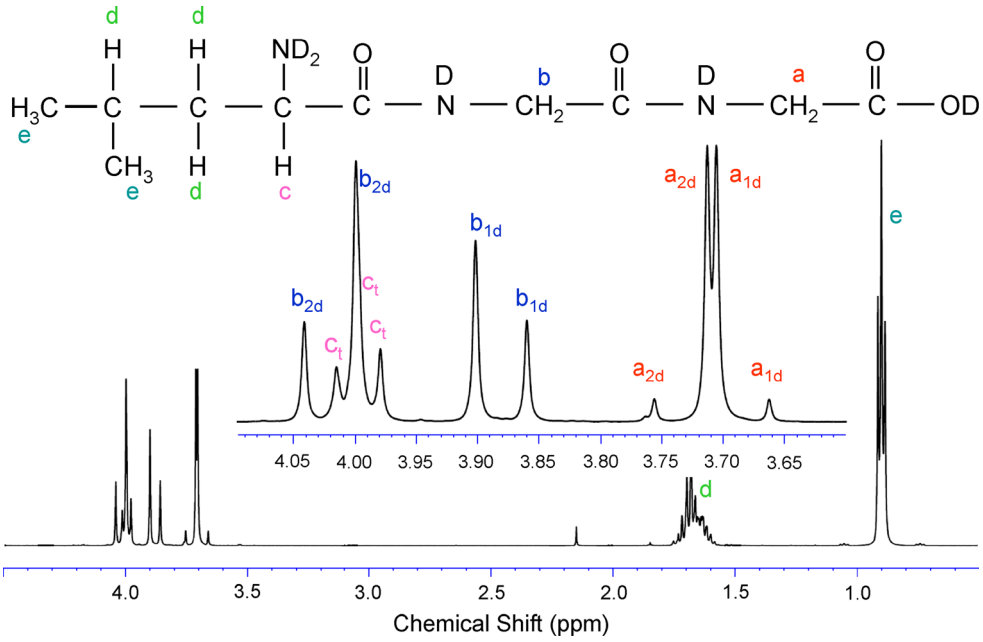

Fig. 1 ^{1}H NMR spectrum of L-Leu-Gly-Gly in D_2O (0.028 mol L^{-1}) at 9.4 T, 25 °C. The central resonances ("a_{1d} and a_{2d}" at 3.71 ppm) were used to form a singlet state in this study

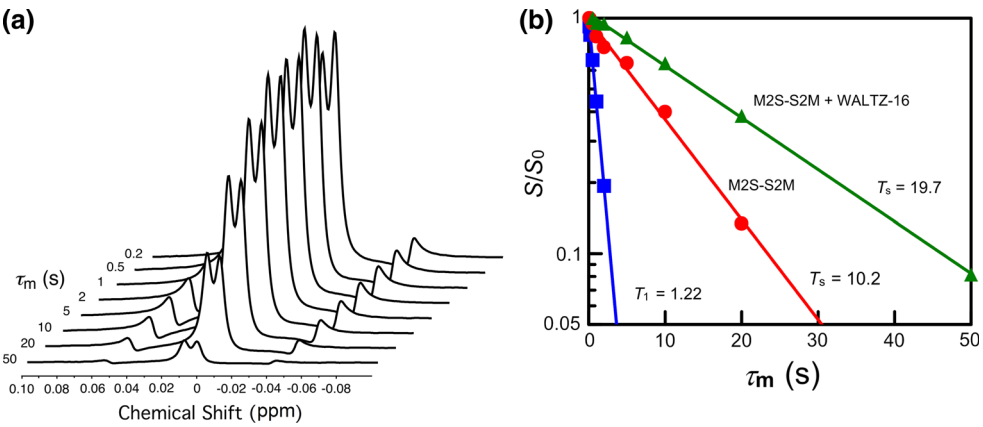

Fig. 2 **a** Stack plot of singlet-state spectra of L-Leu-Gly-Gly solution in D_2O as a function of relaxation interval (τ_m). The M2S-S2M pulse sequence was used to prepare and read out singlet state coherences. **b** Relaxation decay curves of longitudinal magnetization (T_1) and the singlet–triplet population difference (T_s). The latter experiment was repeated with and without WALTZ-16 decoupling during τ_m

resonances of the terminal Gly doublets at 3.71 ppm ("a") were used in this study to form the singlet state. A line shape simulation program based on Levitt's arguments (2011 pp 615–620) yielded parameters of $\Delta\nu = 10.5$ Hz and $J = -17.4$ Hz, which fulfilled the 'strongly coupled' condition $|J| > \Delta\nu$.

Figure 2a shows a stack plot of M2S–S2M spectra of the tripeptide in D_2O. In the measurement, the transmitter offset frequency was set to the center of the doublets. The spectral phase was stable, and all arrays were able to be phase-adjusted using the 0th order and very little 1st order values. With short delays, some instability in the intensity was seen. Figure 2b shows a comparison of the signal decays of longitudinal magnetization and singlet state-triplet state population the difference. Notice that, in M2S–S2M experiments, after the T_0 population has been depleted due to T_1 relaxation, the S_0 state is the only energy level sustaining the magnetization of interest. Therefore, calling the latter magnetization as "a singlet–triplet state population difference" might not be adequate at long time intervals, say more than 1 s in our experiments. Spin coherence was maintained for approximately eight times longer than T_1, without decoupling during the relaxation delay. WALTZ-16 decoupling (Shaka et al. 1983; Freeman 1997) at 0.1 W further increased the relaxation time approximately two fold. The decay curve after more than 1 s of relaxation delay was able to be fitted by a monoexponential function.

The ^{1}H and ^{2}H NMR spectra of a 46 % w/v gelatin hydrogel containing the tripeptide are shown in Fig. 3. The stack plot is presented as a function of extension factor, f_E, from the bottom (original length) to the top (most stretched). The high intensity components of the AB doublets (a_1 and a_2) merged at ~3.65 ppm in the original gel and the signals were re-split as the residual dipolar interaction took effect as a result of stretching the gel further. This is

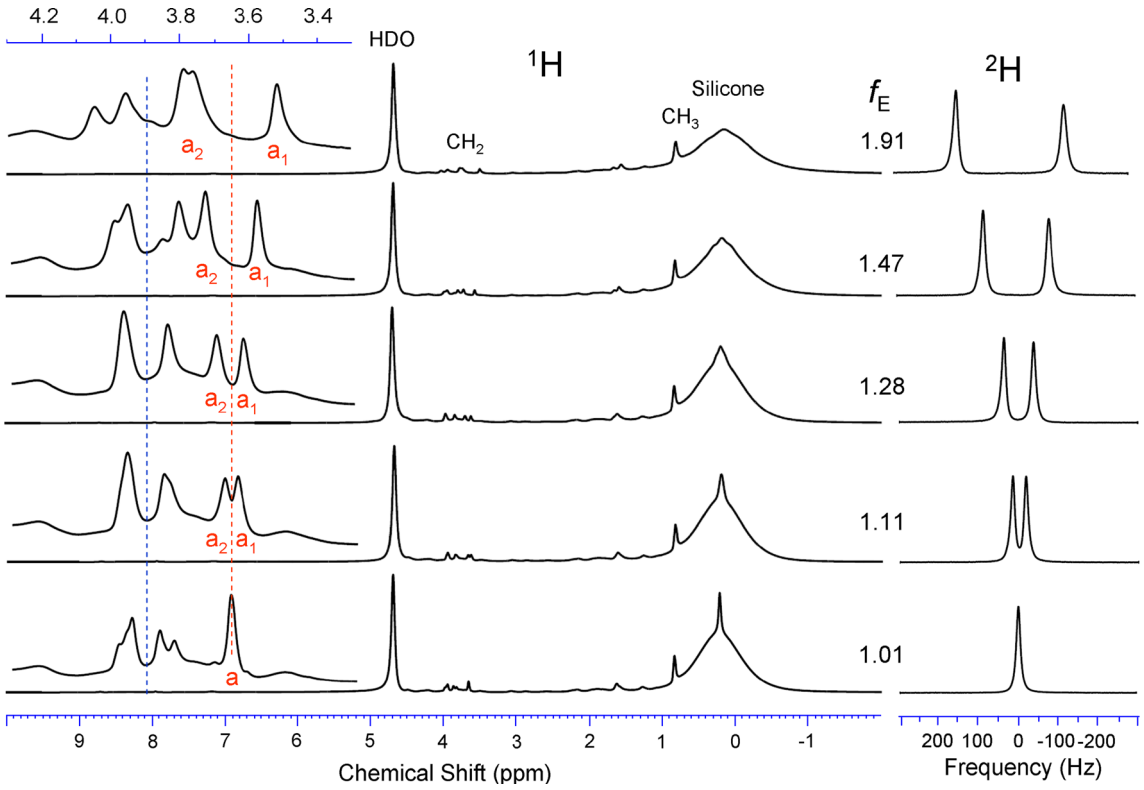

Fig. 3 Stack plot of ^{1}H and ^{2}H NMR spectra of tripeptide/gelatin/D_2O hydrogel as a function of extension factor, f_E. The spectra of gel (46 % gelatin content) in silicone tubing were recorded at 9.4 T and 25 °C, stretching the gel in order to generate anisotropy. The region of interest (3.3–4.3 ppm) is magnified in the left column. All spectra are referenced to the HDO signal specified as 4.70 ppm

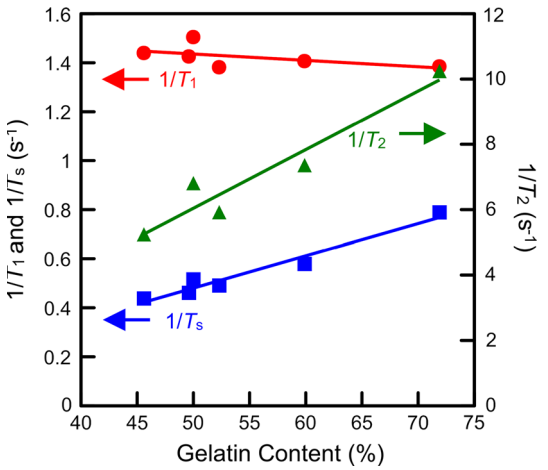

Fig. 4 Relaxation rate constants of geminal CH_2 protons in gelatin as a function of gelatin content (% w/v). The lines were fitted to the data to guide the eye. Notice that the right-hand-side scale for $1/T_2$ is 7.5 times larger than for the left-hand side

due to dipolar interaction superimposed on the *J*-coupling: Residual dipolar interactions cause splitting in a similar way to *J*-coupling. However, residual dipolar splitting between the protons and ^{14}N was negligible in the present spin system. The same extent of splitting was not seen with the ^{1}H in HDO and the CH_3 group of the tripeptide, probably due to their fast exchange and rotational motion, respectively. Although the CH_2 resonance in Fig. 3 appeared to be small compared to the other resonances, the signal-to-noise ratio was sufficient to provide statistically robust parameter estimates.

Figure 4 shows the values of the three relaxation rate constants of the CH_2 protons, as a function of gelatin concentration before stretching the gel. While $1/T_s$ and $1/T_2$ increased with increasing the gelatin concentration, $1/T_1$ decreased. T_s was more sensitive than T_1 to an increase in gelatin concentration, as indicated by the slopes of the fitted lines. This finding is in contrast with the case of a dipeptide in solutions containing lanthanide ions (Tayler and Levitt 2011b) in which T_s was less sensitive than T_1. This effect is consistent with the report by Torres et al. (2012) who observed a significant loss of singlet-state signal from a small organic molecule (5,5′dibromothiophene) at the walls of glass capillaries.

Figure 5 shows the changes in chemical shift, translational diffusion coefficient, T_1, T_2, and T_s versus f_E of a gelatin gel (46 % w/v). The chemical shift of the ^{1}H nuclei in the CH_3 group was almost invariant with f_E, whereas that of the CH_2 group showed a linear dependence in proportion

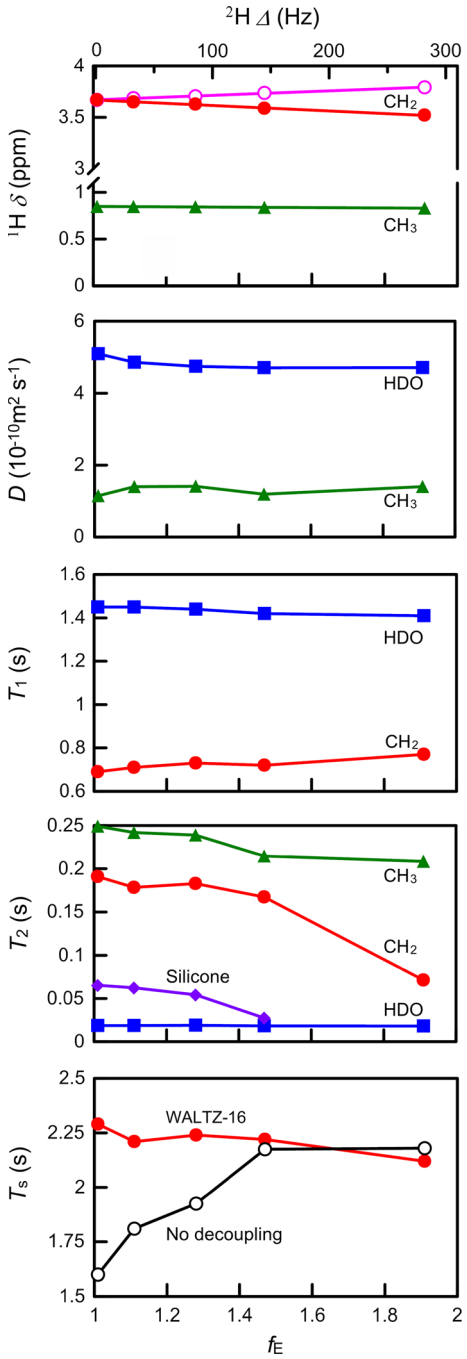

Fig. 5 Changes in NMR parameters as a function of extension factor, f_E, of a stretchable hydrogel prepared at 46 % w/v gelatin content. The diffusion coefficients for the tripeptide were based on the CH_3 signal and the rapidly diffusing components of the intensity profile were extracted by biexponential regression analysis

to the dipolar splitting. The translational diffusion of the peptide in the z-direction (direction of $\mathbf{B}_0$) was not significantly affected by stretching the gel. The same was evident for T_1, implying that the tumbling rate of the molecules in the gel did not significantly change when the gel was stretched. These findings are consistent with the net incompressibility of gel solutions and their contents. The T_2 of the ^{1}H nuclei in the CH_2 and CH_3 groups showed appreciable decreases when the gel was stretched, but T_s only gradually decreased. As the anisotropic molecular alignment progressed, the efficacy of RF-decoupling for extending the singlet-state relaxation time decreased. An increased gel strain might bring the singlet and triplet states closer to the eigenstates of the spin pair as the small chemical shift difference is muffled by a large dipolar splitting.

Discussion

The anisotropic alignment of gel components was manifest in the resonance splittings in our ^{1}H and ^{2}H NMR spectra. The magnitude of the residual quadrupolar splitting $\Delta\nu_Q$ of a ^{2}H signal is given by (Callaghan and Samulski 2003; Li et al. 2008)

$$\Delta\nu_Q = Q\frac{\langle 3\cos^2\theta_{QP} - 1\rangle}{2} \quad (6)$$

where Q is the quadrupolar coupling constant, for which we use 264 kHz for D_2O, as predicted by ab initio calculations (Ludig et al. 1995), and θ_{QP} is the angle between the O-D bond and $\mathbf{B}_0$; thus Eq. (6) is similar to Eq. (4) for dipolar splitting. The apparent alignment angles for the ^{2}H and ^{1}H NMR spectra are plotted in Fig. 6a as a function of f_E. The angles plotted on the ordinate are differences from the magic angle ($\theta_0 = 54.7°$) and the calculated θ_{DP} and θ_{QP}. This value is not an actual angular deviation from the magic angle but it constitutes a measure of stretch-induced anisotropy that is away from the originally isotropic medium. All experimental datasets showed nearly linear relationships with f_E. The calculated angles for the CH_2 protons were ~5 times larger than for the D_2O deuterons; this may be attributed to a difference in the depths of anchoring of the respective molecules into the gelatin network. Recall that only a small net angular bias is necessary to observe the effects of anisotropy in NMR spectra (Levitt 2011 p 446). Figure 6b shows the slopes of the linear fitting as a function of gelatin concentration. The slopes of the various plots pertaining to the ^{1}H nuclei in the CH_2 groups, and the ^{2}H nuclei in D_2O, which reflect how the guests in the gel respond to the alignment, were well correlated with each other. A small divergence occurred above 60 % w/v of gelatin concentration such that a plateau arose in the CH_2 plot while the alignment of the D_2O molecules was not yet saturated. The saturation effect may be consistent with the five-fold larger 'anisotropic angle' of CH_2 than that of D_2O.

Local magnetic field modulations, often referred to as 'fluctuations', lead to nuclear magnetic relaxation.

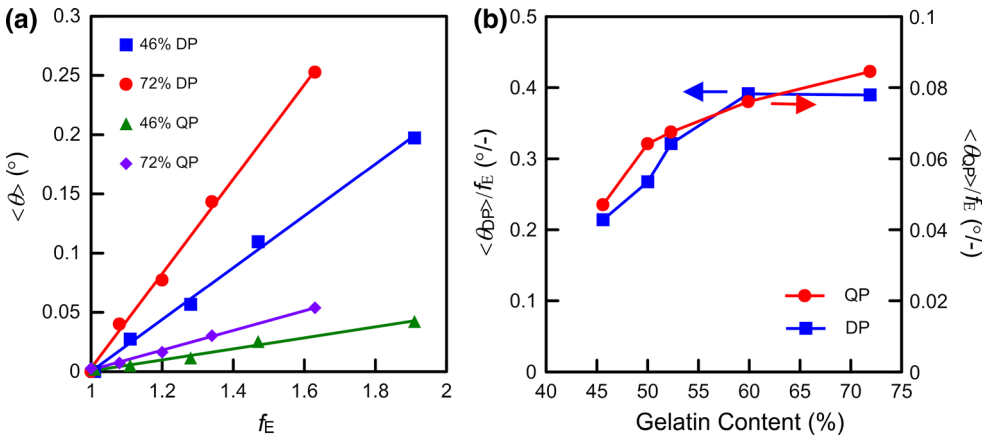

Fig. 6 **a** Calculated alignment angles of the CH_2 of the tripeptide and D_2O in a hydrogel as a function of extension factor, f_E. Experimental results at 46 and 72 % w/v are displayed, where QP indicates the quadrupolar splitting of D_2O, and DP indicates the dipolar splitting of the CH_2 resonance. The plotted angles are differences from the magic angle. The lines were fitted by linear regression. **b** Slopes of the linear fitting of the alignment angles as a function of gelatin content (% w/v)

Modulations in the local magnetic field around a nuclear spin arise from local motions within the spin-bearing molecule, and also from the tumbling of the molecule as a whole. Several mechanisms bring this about: they include dipole–dipole interactions, chemical shift anisotropy, scalar types of the first and second kinds, spin rotation, quadrupolar, and paramagnetic interactions (Harris 1986; Kowalewski and Mäler 2006). In addition to these, and relevant to the relaxation of a singlet state, we revisit the original relaxation theory used to describe the process for isolated spins. The relaxation theory is based on the idea of local random-field fluctuations that are due to random translational motion of molecules in the system, i.e., the zig-zag motion of the spins of interest, and that of the surrounding spin-bearing molecules that exist as the lattice. Depending on the longitudinal and transverse direction of the local random fields, T_1 and T_2 are defined as follows (Harris 1986; Kowalewski and Mäler 2006):

$$\frac{1}{T_1} = \gamma^2 B_x^2 \mathrm{J}_{\mathrm{rnd}}(\omega_0) \tag{7}$$

and

$$\frac{1}{T_2} = \frac{1}{2}\left[\frac{1}{T_1} + \gamma^2 B_z^2 \mathrm{J}_{\mathrm{rnd}}(0)\right] \tag{8}$$

where γ is magnetogyric ratio (rad T^{-1} s^{-1}), B_x^2 and B_z^2 (T^2) are the mean-square local magnetic fields in the perpendicular and parallel directions in the sample relative to the laboratory frame of reference and with respect to $\mathbf{B}_0$, ω_0 is the Lamor angular frequency (rad s^{-1}), and J (s rad^{-2}) is a normalized spectral density function that is given by,

$$\mathrm{J}_{\mathrm{rnd}}(\omega) = \frac{\tau_{\mathrm{rnd}}}{1 + \omega^2 \tau_{\mathrm{rnd}}^2} \tag{9}$$

where τ_{rnd} (s) is the correlation time that describes the loss of magnetization-coherence due to random magnetic field fluctuations. Notice that one part of the expression for $1/T_2$ refers to the same process as T_1 relaxation, while the other part accounts for local magnetic field fluctuations, as projected into the z-direction. Isotropic random field events of unspecified origin are often ignored in calculations of relaxation rate constants because B_x and B_z are typically small compared with fluctuations caused by molecular motion. However, the effect is not negligible for the relaxation of singlet states as the dipolar effect is muffled (Carravetta and Levitt 2011). If we assume non-coupled isolated spins surrounded by a lattice, it is predicted from Fig. 5 and Eqs. (7–9) that stretching the gel would not bring about a significant change in correlation time. The change in T_2 would then be attributable to the increase in B_z^2 caused by the anisotropic alignment. However, this argument is still only intuitive and may not apply in gel systems in which dipolar interactions are not averaged when the gel is stretched.

Intramolecular dipolar spin relaxation is well known to be described by a linear combination of Lorentzian spectral density functions that in turn describe relaxation that occurs via zero-, single-, and double-quantum transitions (Bloembergen et al. 1948; Abragam 1961; McConnell 1987):

$$\begin{aligned} \frac{1}{T_1^{\mathrm{DD}}} &= \frac{3}{10} b^2 [\mathrm{J}_{\mathrm{DD}}(\omega_0) + 4\,\mathrm{J}_{\mathrm{DD}}(2\omega_0)] \\ \frac{1}{T_2^{\mathrm{DD}}} &= \frac{3}{20} b^2 [3\,\mathrm{J}_{\mathrm{DD}}(0) + 5\,\mathrm{J}_{\mathrm{DD}}(\omega_0) + 2\,\mathrm{J}_{\mathrm{DD}}(2\omega_0)] \end{aligned} \tag{10}$$

where b (rad s^{-1}) is the dipolar coupling constant defined by Eq. (4), and $\mathrm{J}_{\mathrm{DD}}(\omega)$ is a spectral density function defined for dipolar relaxation in the same format as Eq. (9).

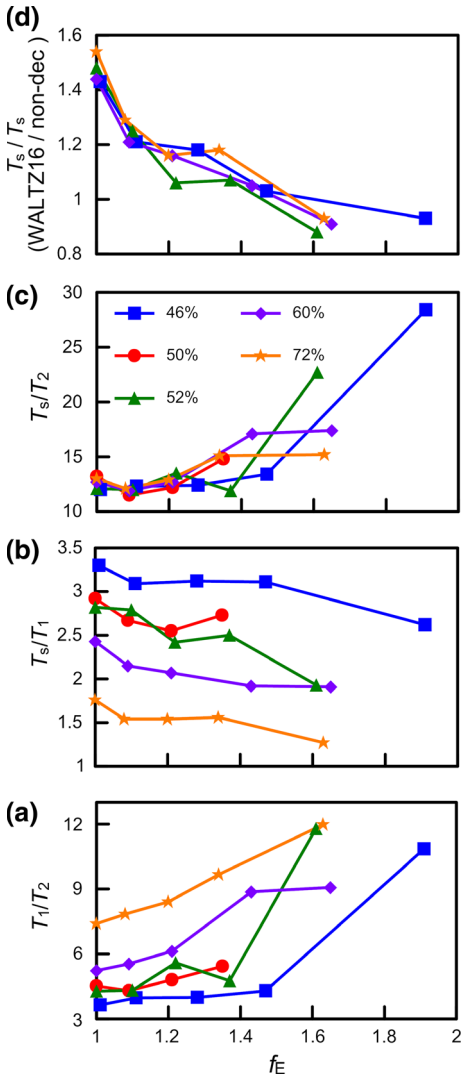

Fig. 7 Ratios of relaxation time constants measured at different gelatin contents as a function of extension factor, f_E. This one figure contains all experimental data points acquired in this study

If intramolecular dipolar interactions are assumed to be the only source of relaxation, a correlation time τ_{DD} (s rad^{-1}) can be calculated from the ratio T_1/T_2 (Carper and Keller 1997; Bakhmutov 2004):

$$\tau_{DD} = \frac{1}{2\sqrt{6}\,\omega_0} \sqrt{-37 + 16(T_1/T_2) + \sqrt{889 - 704(T_1/T_2) + 256(T_1/T_2)^2}} \tag{11}$$

The graph of the correlation times calculated from Eq. (11) plotted versus f_E, was of almost the same appearance as the plot of T_1/T_2 in Fig. 7a, except for the scale and label on the ordinate. The T_s/T_1 ratio of 3.3 was the highest relaxation time gain with use of WALTZ-16 decoupling during relaxation delays. This gain in relaxation time is comparable with results of ^{1}H singlet-states achieved in the extreme narrowing limit in the presence of paramagnetic ions (Tayler and Levitt 2011b). The curves for T_s/T_2 and T_s/T_s for the use and nonuse of broadband decoupling appeared to overlap regardless of gelatin concentration and value of f_E.

Pertinent to this finding is Carravetta and Levitt's (2005) equation for singlet state relaxation time:

$$\frac{1}{T_s} \simeq \frac{1}{2}\left(3A_1 + 2A_2 + 3A_3 - \sqrt{9A_1^2 + 4A_2^2 + 9A_3^2 - 4A_1A_2 - 14A_1A_3 - 4A_2A_3}\right) \tag{12}$$

where

$$\begin{aligned} A_1 &= \frac{1}{20}\left[5\gamma^2(B_j^2 + B_k^2 - 2C_{jk}B_jB_k\cos\xi)\,J_{rnd}(\omega_0) + 3\,b^2 J_{DD}(\omega_0)(1-\cos\xi)\right] \\ A_2 &= \frac{1}{20}\left[5\gamma^2(B_j^2 + B_k^2 - 2C_{jk}B_jB_k)\,J_{rnd}(0)\cos^2\xi + 2\,b^2 J_{DD}(0)\sin^2\xi\right] \\ A_3 &= \frac{1}{20}\left[5\,\gamma^2(B_j^2 + B_k^2 + 2C_{jk}B_jB_k\cos\xi)\,J_{rnd}(\omega_0) + 2\,b^2 J_{DD}(\omega_0)(1+\cos\xi)\right] \end{aligned} \tag{13}$$

Thus Eq. (12) is a combination of a random field relaxation term and a dipolar relaxation term. The B_j and B_k terms are root-mean-square local random fields that affect the j and k spins; and this interaction is correlated, as expressed in the coefficient C_{jk}. Spectral density functions (J_{rnd} and J_{DD}) are separately defined for both the random field and dipolar interactions. The b term is the dipolar coupling constant, as given in Eq. (4), and ξ is the singlet–triplet mixing angle defined by $\xi = \arctan(\Delta\nu/J)$. The T_1, T_2 and T_s curves at 9.4 T are plotted in Fig. 8, in which the correlation times were assumed to be the same for the random and dipolar fields ($\tau_{rnd} = \tau_{DD}$). Unknown parameters in this expression are B_j, B_k, and C_{jk} while all other physical parameters can be fixed, from the geometrical information of the geminal proton pair of the tripeptide. The magnitude of the random and dipolar fields [B_j, B_k and b in Eq. (13)] control the up-down movement of the curves. The minimum of the T_1 curve is at $\tau_{rnd} = 1/\omega_0$ for a random field, and at $\tau_{DD} = 0.6158/\omega_0$ for the dipolar case, so the difference constitutes the window of horizontal movement of the T_s curve. As shown in Fig. 8a, the assumption of dipolar relaxation underestimates the effect seen in the experimental data for all three relaxation times, but the order of values and the trend of changes were reproducible. The ratios of the relaxation times given in Fig. 8b were more consistent with the experimental data. The estimated

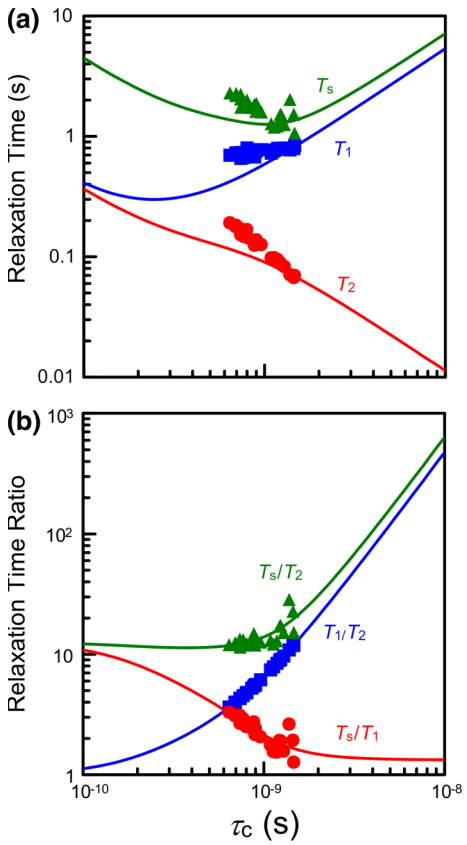

Fig. 8 Theoretical fitting of all experimental relaxation data as a function of calculated correlation times. The theoretical predictions are drawn with solid lines. The T_1 and T_2 relaxation processes were assumed to be purely through intramolecular dipolar interactions; and the correlation time was calculated from the T_1/T_2 ratio as explained in Eq. (11). **a** Experimental relaxation time constant data as a function of calculated correlation time. **b** The ratios of experimental relaxation time constants plotted against calculated correlation times. The T_s relaxation-time-constant curve was calculated with random field strength $B_j = B_k = 155$ μT at their correlation $C_{jk} = 0.91$ and the dipolar coupling constant $b = -22.3$ kHz

maximum value of T_s/T_1 was as high as 10.8 for our gel system; this appears to be within a reasonable range because the value in free solution given in Fig. 2b was 16.1. T_s/T_1 values should be increased or decreased depending on the choice of gel materials and singlet-forming molecules. A gain of greater than 1.33 is always expected for T_s/T_1 with the present gelatin-tripeptide combination, as a plateau exists at high correlation times (slow motion). The overlapping of experimental T_s/T_2 curves in Fig. 7c is thus posited to be due to the presence of a plateau in the low correlation time regime in Fig. 8b around $\tau_c < 10^{-9}$ (s rad^{-1}). With respect to Fig. 7d, the overlap of plots for different gelatin concentrations was concluded to be due to cancellation of intermolecular dipolar interactions by using broadband decoupling. When the gelatin concentration was increased more, relaxation sources emerged in direct proportion. A reduction of the effect of decoupling with stretching the gel was concluded to be due to molecular alignment with its attendant increase in intramolecular dipolar interactions; such strong interactions are no longer averaged by standard liquid NMR decoupling techniques. Actually, even if decoupling is used, some leakage from $ZQ_x = (1/2)\ (|T_0\rangle\langle T_0| - |S_0\rangle\langle S_0|)$ is always taking place due to imperfect cancellation of chemical shift differences by WALTZ decoupling (Gopalakrishnan and Bodenhausen 2006; Pileio and Levitt 2009). An experimentally observed T_s value should have significance as long as it is larger than T_1 because the time gain can be exploited for preserving hyperpolarized magnetization, detecting slow diffusion, or rendering MRI contrast. For in vivo applications of singlet states, SAR (surface absorption rate) of radio frequency waves by animal or human body must always be considered. Then, we would probably have to use the M2S–S2M sequence without decoupling.

Finally, we cannot clearly envisage at this stage how practical in vivo singlet MR would become in the future. Although it is not implausible (cf. DeVience et al. 2013; Pileio et al. 2013), it would be still technically challenging. Muscles do not have an appreciable amount of tripeptides in it. However, a probe molecule for detecting a singlet state need not be a tripeptide; it could be a dipeptide, ATP, creatine, or glycogen as long as asymmetric spin states can be formed within its nuclei. Also, singlet-forming spin pairs do not have to exist in tissues essentially from the original state. For example, hyperpolarized glucose (Allouche-Arnon et al. 2013) can be injected into muscle or fibrous tissues. Besides, ^{31}P NMR of chemical shifts muscle in a magnetic field depend on the orientation with respect to $\mathbf{B_0}$ if stretched and relaxed (Prompers et al. 2006). Standard ^{1}H imaging of fluids or tissues based on T_1 or T_2 weighting does not give dynamic information on metabolism, so ^{31}P singlet-state methods combined with dynamic nuclear polarization may be a good way to study it.

Conclusions

NMR singlet states were observed in a viscous gelatin medium in which T_2 was significantly less than T_1. The tripeptide, L-Leu-Gly–Gly, in gelatin gel was studied by using the M2S-S2M sequence with WALTZ-16 decoupling. The observation of the singlet state exploited the echo-train pulse sequence advocated for strongly coupled proton pairs ($\Delta\nu < J$); we also used well defined and calibrated timing and loop parameters, and only moderate broadband decoupling power. Prolongation of relaxation times by use of singlet states was observed even in the aligned medium showing residual dipolar coupling. In a hydrogel, T_s became

T_2-sensitive, which is a new finding for a long-lived state that has not been so far studied outside of the extreme narrowing regime. Our findings could help pave the way to in vivo singlet state studies of fibrous and extensible tissues such as nerves and muscles, respectively.

References

Abragam A (1961) Principle of nuclear magnetism. Oxford University Press, Oxford, pp 289–292

Aguilar JA, Nilsson M, Bodenhausen G, Morris GA (2012) Spin echo spectra without J-modulation. Chem Commun 48:811–813

Allouche-Arnon H, Wade T, Waldner LF, Miller VN, Gomori JM, Katz-Brull R, McKenzie CA (2013) In vivo magnetic resonance imaging of glucose: initial experience. Contrast Media Mol Imaging 8:72–82

Bakhmutov VI (2004) Practical NMR relaxations for chemists. John Wiley & Sons Ltd, Chichester, pp 170–172

Barfield M, Hruby VJ, Meraldi J-P (1976) The dependence of geminal H–H spin–spin coupling constants on ϕ and ψ angles of peptides in solution. J Am Chem Soc 98:1308–1314

Bax A (2003) Weak alignment offers new NMR opportunities to study protein structure and dynamics. Protein Sci 12:1–16

Bloembergen N, Purcell EM, Pound RV (1948) Relaxation effects in nuclear magnetic resonance absorption. Phys Rev 73:679–712

Callaghan PT, Samulski ET (2003) Biaxial deformation of a polymer network measured via deuteron quadrupolar interactions. Macromolecules 36:724–735

Carper WR, Keller CE (1997) Direct determination of NMR correlation times from spin-lattice and spin–spin relaxation times. J Phys Chem A 101:3246–3250

Carravetta M, Levitt MH (2005) Theory of long-lived nuclear spin states in solution nuclear magnetic resonance. I. Singlet states in low magnetic field. J Chem Phys 122:214505

Carravetta M, Johannessen OG, Levitt MH (2004) Beyond the T_1 Limit: singlet nuclear spin states in low magnetic fields. Phys Rev Lett 92:15303

Chen L, Longenecker JG, Moore EW, Marohn JA (2013) Magnetic resonance force microscopy detected long-lived spin magnetization. IEEE Trans Magn 49:3528–3532

DeVience SJ, Walsworth RL, Rosen MS (2013) Nuclear spin singlet states as a contrast mechanism for NMR spectroscopy. NMR Biomed 26:1204–1212

Feng Y, Davis RM, Warren WS (2012) Accessing long-lived nuclear singlet states between chemically equivalent spins without breaking symmetry. Nature Phys 8:831–837

Franzoni MB, Buliubasich L, Spiess HW, Münnemann K (2012) Long-lived ^{1}H singlet spin states originating from para-hydrogen in Cs-symmetric molecules stored for minutes in high magnetic fields. J Am Chem Soc 134:10393–10396

Freeman R (1997) A handbook of nuclear magnetic resonance, 2nd edn. Addison Wesley Longman Ltd, Harlow, pp 20–30

Ghosh RK, Kadlecek SJ, Ardenkjaer-Larsen JH, Pullinger BM, Pileio G, Levitt MH, Kuzma NN, Rizi RR (2011) Measurements of the persistent singlet state of N_2O in blood and other solvents: potential as a magnetic tracer. Magn Reson Med 66:1177–1180

Gopalakrishnan K, Bodenhausen G (2006) Lifetimes of the singlet-states under coherent off-resonance irradiation in NMR spectroscopy. J Magn Reson 182:254–259

Hallwass F, Schmidt M, Sun H, Mazur A, Kummerlöwe G, Luy B, Navarro-Vázquez A, Griesinger C, Reinscheid UM (2011) Residual chemical shift anisotropy (RCSA): a tool for the analysis of the configuration of small molecules. Angew Chem Int Ed 50:9487–9490

Harris RK (1986) Nuclear magnetic resonance spectroscopy: a physicochemical view. Longman Scientific & Technical, Harlow, pp 84–95

Hoffman RA, Forsén S, Gestblom G (1971) Analysis of NMR spectra. In: Diehl P, Fluck E, Kosfeld R (eds) NMR basic principles and progress, vol 5. Springer-Verlag, Berlin, p 142

Kowalewski J, Mäler L (2006) Nuclear spin relaxation in liquids: theory experiments, and applications. Taylor & Francis Group, Boca Raton, pp 19–38

Kuchel PW, Chapman BE, Müller N, Bubb WA, Philp DJ, Torres AM (2006) Apparatus for rapid adjustment of the degree of alignment of NMR samples in aqueous media: verification with residual quadrupolar splittings in ^{23}Na and ^{133}Cs spectra. J Magn Reson 180:256–265

Kummerlöwe G, Luy B (2009) Residual dipolar coupling for the configurational and conformational analysis of organic molecules. Annu Rep NMR Spectrosc 68:193–232

Kummerlöwe G, Halbach F, Laufer B, Luy B (2008) Precise measurement of RDCs in water and DMSO based gels using a silicone rubber tube for tunable stretching. The Open Spectrosc J 2:29–33

Laustsen C, Pileio G, Tayler MCD, Brown LJ, Brown RCD, Levitt MH, Ardenkjaer-Larsen JH (2012) Hyperpolarized singlet NMR on a small animal imaging system. Magn Reson Med 68:1262–1265

Levitt MH (2011) Spin dynamics: basics of nuclear magnetic resonance, 2nd edn. John Wiley & Sons Ltd, Chichester

Levitt MH (2012) Singlet nuclear magnetic resonance. Annu Rev Phys Chem 63:89–105

Li J, Wilmsmeyer KG, Madsen LA (2008) Hydrophilic alignment modes in perfluorosulfonate ionomers: implications for proton transport. Macromolecules 41:4555–4557

Ludig R, Weinhold F, Farrar TC (1995) Experimental and theoretical determination of the temperature dependence of deuteron and oxygen quadrupole coupling constants of liquid water. J Chem Phys 103:6941–6950

McConnell J (1987) The theory of nuclear magnetic relaxation in liquids. Cambridge University Press, Cambridge, pp 47–60

Naumann C, Bubb WA, Chapman BE, Kuchel PW (2007) Tunable-alignment chiral system based on gelatin for NMR spectroscopy. J Am Chem Soc 129:5340–5341

New Era Enterprises Inc (2012–2013) NMR Catalog 12–13, pp 18–22

Pelta MD, Barjat H, Morris GA, Davis AL, Hammond SJ (1998) Pulse sequences for high-resolution diffusion-ordered spectroscopy (HR-DOSY). Magn Reson Chem 36:706–714

Pileio G, Levitt MH (2009) Theory of long-lived nuclear spin states in solution nuclear magnetic resonance. II. Singlet spin locking. J Chem Phys 130:24501

Pileio G, Carravetta M, Levitt MH (2010) Storage of nuclear magnetization as long-lived singlet order in low magnetic filed. Proc Natl Acad Sci USA 107:17135–17139

Pileio G, Bowen S, Laustsen C, Tayler MCD, Hill-Cousins JT, Brown LJ, Brown RCD, Ardenkjaer-Larsen JH, Levitt MH (2013) Recycling and imaging of nuclear singlet hyperpolarization. J Am Chem Soc 135:5084–5088

Prompers JJ, Jeneson JAL, Drost MR, Oomens CCW, Strijkers GJ, Nicolay K (2006) Dynamic MRS and MRI of skeletal muscle function and biomechanics. NMR Biomed 19:927–953

Reich HJ (2013) Chem 605: structure determination using spectroscopic methods, 5.10 AX and AB Spectra, http://www.chem.wisc.edu/areas/reich/nmr/. Accessed 13 Dec 2013

Shaka AJ, Keeler J, Frenkiel T, Freeman R (1983) An improved sequence for broadband decoupling: WALTZ-16. J Magn Reson 52:335–338

Tayler MCD, Levitt MH (2011a) Singlet nuclear magnetic resonance of nearly-equivalent spins. Phys Chem Chem Phys 13:5556–5560

Tayler MCD, Levitt MH (2011b) Paramagnetic relaxation of nuclear singlet states. Phys Chem Chem Phys 13:9128–9130

Tayler MCD, Marco-Rius I, Kettunen MI, Brindle KM, Levitt MH, Pileio G (2012) Direct enhancement of nuclear singlet order by dynamic nuclear polarization. J Am Chem Soc 134:7668–7671

Tonan K, Ikawa S (2003) Effect of solvent on an NMR chemical shift difference between glycyl geminal α-protons as a probe of β-turn formation of short peptides. Spectrochim Acta, Part A 59:111–120

Torres AM, Ghadirian B, Price WS (2012) Diffusion–diffraction using singlet spin states and various NMR coherences in a J-coupled AX spin system. RSC Advances 2:3352–3360

Vasos PR, Comment A, Sarkar R, Ahuja P, Jannin S, Ansermet JP, Konter JA, Hautle P, van den Brandt B, Bodenhausen B (2009) Long-lived states to sustain hyperpolarized magnetization. Proc Proc Natl Acad Sci USA 106:18469–18473

Warren WS (2011) Magnetic resonance imaging and/or spectroscopy contrast agents and methods of use thereof. US Patent Application 0192058 A1

Wu DH, Chen AD, Johnson CS Jr (1995) An improved diffusion-ordered spectroscopy experiment incorporating bipolar-gradient pulses. J Magn Reson A 115:260–264

Zhang B, Lee JS, Khitrin A, Jerschow A (2013) Long lived NMR signal in bone. J Magn Reson 231:1–4